

## Inhomogeneous ferromagnetic ordering in *PdFe* and *PdMn* alloys studied via small-angle neutron scattering

B. H. Verbeek,\* G. J. Nieuwenhuys, and J. A. Mydosh

*Kamerlingh Onnes Laboratorium der Rijksuniversiteit, Leiden, The Netherlands*

C. van Dijk

*Netherlands Energy Research Foundation ECN, Petten (N.-H.), The Netherlands*

B. D. Rainford

*Department of Physics, The University, Southampton, United Kingdom*

(Received 24 March 1980)

The results of small-angle ( $0.025 < Q < 0.125 \text{ \AA}^{-1}$ ) neutron scattering measurements on dilute ferromagnetic *PdFe* (0.25, 0.5, 1, and 2 at. %) and *PdMn* (0.5 and 2 at. %) alloys are presented. Critical scattering has been clearly observed in a wide temperature interval around the Curie temperature, which for  $T > T_C$  could be described by the usual Ornstein-Zernike formalism, but for  $T < T_C$  exhibited an extra quasicohherent scattering. Both the temperature and magnetic field dependence of this additional scattering could be explained by the presence of randomly oriented ferromagnetic clusters or microdomains. It is found that a distribution of cluster sizes is necessary to describe the observed scattering. The induced magnetic polarization associated with the individual giant moments in *PdFe* is obtained from the anisotropic scattering in a magnetic field and gave an average spatial extent of about  $50 \text{ \AA}$ . A comparison of the macroscopic magnetization and the neutron scattering results is made. A modified percolation type of model has been employed to describe the ferromagnetic ordering process, and evidence is provided that the giant moment systems can be characterized as a special case among the more general spin-glass systems.

### I. INTRODUCTION

Random dilute alloys exhibit a variety of interesting phenomena for different concentrations of magnetic impurities.<sup>1,2</sup> If single, localized magnetic impurities are considered with indirect couplings via the conduction electrons, then, in general, two types of magnetic order can be distinguished in these alloys: "giant-moment ferromagnetism" and "spin-glass freezing." The term giant moment describes the behavior which results from substituting an impurity in a nonmagnetic, but exchange enhanced, host metal, and thereby producing a magnetic moment per impurity much larger than that due to the bare magnetic impurity alone. This overall magnetic moment is composed of the single, localized moment plus an induced moment in the surrounding host metal. Such magnetic entities can be considered as one magnetic moment which is then called *giant*. Good examples of giant-moment systems are Pd alloys with small amounts ( $c < 2$  at. %) of Fe, Co, or Mn.<sup>3</sup> Magnetic moments up to  $12\mu_B$  have been observed in *PdFe* alloys of which about  $8\mu_B$  is distributed among the surrounding Pd ions. This increase of in-

teraction range leads to a ferromagnetic ordering in these alloys with concentrations  $c \geq 0.1$  at. % which is far below a critical concentration for direct (nearest-neighbor) interactions. The concept of percolation as introduced in the spin-glass systems by Smith<sup>4,5</sup> will be adopted to give a meaningful description of the ordering in the ferromagnetic giant-moment systems.

Magnetic diffuse neutron scattering has been widely used to study the microscopic magnetic properties of alloys and, in particular, has shown that all ferromagnetic alloys are magnetically inhomogeneous. In general the variation of magnetic moment with composition can be very complex involving the effects of chemical clustering.<sup>6,7</sup> However, if the concentration of impurities is sufficiently small and good local moments are available, the magnetic scattering is predominantly determined by identical scattering centers. For the giant-moment systems the angular distribution of the scattered neutrons is then related to the giant-moment complex. Indeed, the diffuse scattering results by Low *et al.*<sup>8,9</sup> on *PdFe* and *PdCo* alloys has revealed an additional scattering in the forward direction which has been attributed to the induced Pd polarization. However, in view of the

present results, we must conclude that this additional scattering contribution contains both critical scattering as well as a quasicohherent contribution due to the inhomogeneous ferromagnetic state of the alloys. In these early experiments<sup>8,9</sup> the scattering cross sections were measured at large  $Q$  values ( $\geq 0.2 \text{ \AA}^{-1}$ ) with a  $Q$  resolution of  $\approx \pm 0.15 \text{ \AA}^{-1}$  which did not permit a fine separation of the various scattering contributions. Indications for the additional scattering mechanism in the small-angle region came from similar diffuse neutron scattering studies on Pd Mn alloys<sup>10,11</sup> where the scattering in the forward direction did not extrapolate to the value prescribed by the saturation magnetization. A detailed investigation of the small-angle scattering of some Pd Fe and Pd Mn alloys was then performed to elucidate this anomalous behavior. A preliminary report on this work has been published.<sup>12</sup>

In Sec. II experimental details and data reduction will be outlined. The experimental results of the temperature and magnetic field dependence of the small-angle scattering are given in Sec. III. Section IV contains the anisotropic scattering results for some Pd Fe alloys due to an external magnetic field and these will be related to measurements of the macroscopic magnetization on the same samples. An interpretation of the results and a description of the cluster ordering in these alloys in terms of a modified percolation model is presented in Sec. V.

## II. EXPERIMENTAL DETAILS

Measurements have been carried out on nominal concentration Pd Mn 0.5 and 2 at. % and Pd Fe 0.25, 0.5, 1, and 2 at. %. The samples were prepared by induction melting the appropriate amounts of Pd [Johnson-Mathey (JM) 6-9], Fe (JM4-9), and Mn (JM4-9) in an argon atmosphere, followed by annealing at 800 °C for 4 h and furnace cooling. From the ingots, cylinders were made with a diameter of 15 mm and thickness of 6 mm via spark erosion. The impurity concentrations of the alloys have been determined chemically and gave Pd Mn 0.45 and 2.1 at. % and Pd Fe 0.27, 0.48, 0.95, and 2.2 at. %.

Small-angle neutron scattering measurements have been performed with the small-angle camera D11A at the High Flux Reactor, Institute Laue-Langevin in Grenoble. A neutron wavelength of 6.28 Å has been employed and the distance between sample and multidetector was 2.5 m, resulting in an effective  $Q$  range of 0.025 to 0.125 Å<sup>-1</sup>, with a spatial resolution of  $\Delta Q \approx 3 \times 10^{-3} \text{ \AA}^{-1}$ . The samples were mounted in the tail of a flow cryostat in which the temperature could be controlled between 2.5 K and room temperature within 0.1 K during runs of typical 30 min. The temperature was measured using a calibrated Si diode. A cadmium shield was used to reduce back-

ground scattering from the sample holder.

All metallic systems show small-angle scattering due to metallurgical properties such as grains, dislocations, voids, surface contaminations, etc., which may vary from sample to sample. In order to obtain the isotropic magnetic contribution the correction for nuclear and background scattering has been made by taking a high-temperature measurement, where magnetic correlations are not important. All low-temperature and field dependent scattering due to magnetic interactions are obtained by subtracting this high-temperature spectrum from the spectra in the temperature range of interest. In most cases this background spectrum has been measured at or just below room temperature. However, this experimental method is insufficient to obtain the magnetic diffuse scattering which is associated with the individual giant moments. Here careful correction and calibration procedures are required to analyze the raw data taken in a magnetic field of 0.36 T by exploiting the anisotropic character of the diffuse magnetic scattering in a field. The background is determined in two ways with an empty sample holder and with a pure Pd sample under identical conditions as the actual experiment, while the correction for fast neutrons is done by placing a cadmium shield in front of the sample. The absorption correction is usually calculated with tabulated cross sections and compared with the results of transmission experiments. From careful transmission experiments on pure Pd and Pd Mn alloys with neutron wavelengths of 2.58 and 4.04 Å, we have now obtained an absorption cross section for Pd of  $\sigma_a = 5.2 \pm 0.5 \text{ b}$  at  $\lambda = 1.8 \text{ \AA}$  (thermal neutrons) which is smaller than the value quoted in the literature of  $\sigma_a = 6.9 \pm 0.4 \text{ b}$  at  $\lambda = 1.8 \text{ \AA}$ .<sup>13</sup> A detector efficiency correction has been applied to the anisotropic scattering data since the individual counting cells of the multidetector possess variations in counting efficiency. The efficiency has been measured using the strong, isotropic, incoherent scatterer, polystyrene. The normalized detector efficiency for every cell has been used to correct all cells of the sample spectra. After having applied the corrections, the data are normalized on an absolute cross-section scale by comparing with the intensity obtained from a 3-mm-thick vanadium standard corrected for multiple scattering and background.

## III. EXPERIMENTAL RESULTS

### A. Temperature and magnetic field dependence of the magnetic scattering

The temperature dependence of the magnetic scattering for various  $Q$  values in zero magnetic field of Pd Mn 2 at. %, Pd Fe 0.25 and 0.5 at. % are shown

in Figs. 1, 2, and 3. These results clearly demonstrate<sup>12</sup> that these random dilute alloys show pronounced critical scattering at a well-defined Curie temperature, and thus show the onset of long-range ferromagnetic order. The scattering intensities exhibit two distinct features which may be taken as typical for dilute magnetic systems. The first is the strong  $Q$  dependence of the critical scattering where for the smallest  $Q$  a divergence in the scattering intensity seems to appear, but for  $Q$  values larger than  $0.1 \text{ \AA}^{-1}$  only a small rounded maximum is visible near the Curie temperature. Such a rounded maximum has also been observed in the temperature dependence of the diffuse magnetic scattering from *Pd Mn 0.46 at. %*.<sup>11</sup> Therefore, we must conclude from the present results that critical scattering plays an important role in the enhanced forward scattering in the *Pd Mn 0.23* and *0.46 at. %* alloys.

The second remarkable feature of the scattering intensities is the wide temperature range in which critical effects are observed. As a rule of thumb, homogeneous systems with a magnetic phase transition exhibit critical scattering only in a temperature range of approximately 10% of the transition temperature.

However, in the *Pd Mn* and *Pd Fe* alloys critical effects are observed at temperatures far above and far below the Curie temperature.

Two explanations may be proposed to account for this behavior. Firstly a qualitative argument can be made based upon the  $Q$ -dependent susceptibility in a

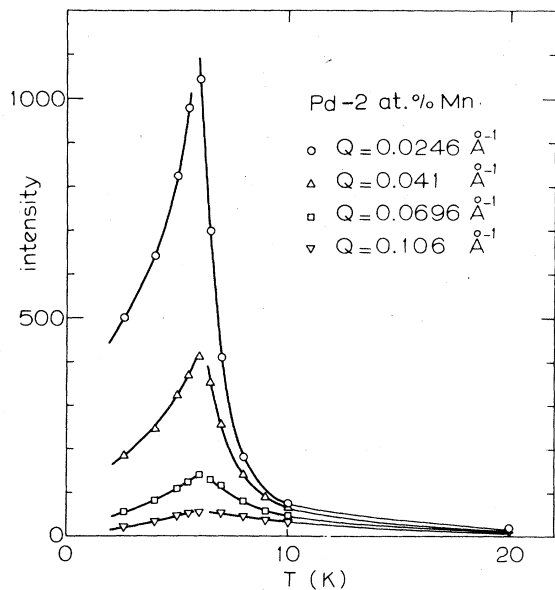


FIG. 1. Small-angle neutron scattering intensity vs temperature of *Pd-2 at. % Mn* for various  $Q$  values.

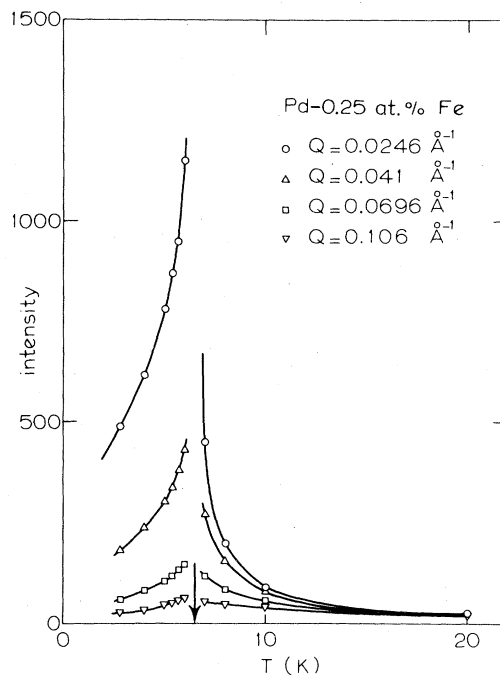


FIG. 2. Neutron scattering intensity vs temperature for *Pd-0.25 at. % Fe* for various  $Q$  values. The arrow indicates the Curie temperature.

mean-field description of the critical scattering<sup>14</sup>

$$\chi(Q) = \frac{\chi_C}{(T - T_C)/T_C + [1 - J(Q)/J(0)]} \quad (1)$$

which may be approximated by the well-known

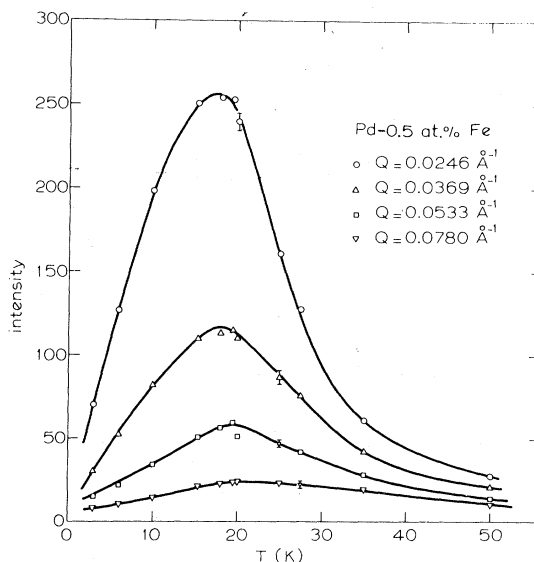


FIG. 3. Neutron small-angle scattering of *Pd-0.5 at. % Fe* vs temperature for various  $Q$  values.

Lorentzian

$$\chi(Q) = \frac{\chi_C}{R^2(Q^2 + \kappa_1^2)}, \quad (2)$$

where for  $T > T_C$ :  $R^2 = \frac{1}{6} J^{(2)}/J(0) = R_{NN}^2/6$  for nearest-neighbor impurities,  $\kappa_1$  is the inverse correlation length  $\kappa_1^2 = (T - T_C)/(T_C R^2)$  and  $\chi_C$  is the Curie susceptibility. For a dilute system one can estimate  $R_{NN}$  as the mean distance between the impurity atoms given in Ref. 15 for fcc lattices

$$R_{NN} = 0.34 a_0 c^{-1/3}, \quad (3)$$

where  $c$  is the fraction of impurities and  $a_0$  the lattice parameter. The mean distance is relatively large—a few lattice constants—so that the inverse correlation length,  $\kappa_1$ , remains small over a wide temperature range.

The second explanation, which anticipates a more general conclusion about the ferromagnetic ordering in these systems, involves the presence of clusters of giant moments due to the random, statistical distribution of impurities in the host. These clusters or correlated magnetic regions, which give rise to the small-angle scattering, may be formed at temperatures much higher than the Curie temperature, since this temperature only indicates the onset of the long-range order, e.g., hysteresis effects in the magnetization have been observed by us at temperatures  $T \approx 5 T_C$  for Pd Co and Pd Fe. From Figs. 1–3 it is clear that, especially on the low-temperature side, the scattering intensity remains unusually large to be simply attributed to critical scattering. Indeed, an extra magnetic contribution is present at low temperatures which can be shown to be much more pronounced in the following way. If the expression for critical magnetic scattering [Eq. (1)] holds for dilute systems, then the scattering intensity is given by

$$I(Q) \propto F^2(Q) T \chi(Q), \quad (4)$$

where  $F(Q)$  is the magnetic form factor. The divergence in the scattering intensity is determined by the divergence in the wave-vector-dependent susceptibility  $\chi(Q)$  and, therefore, the true critical scattering can be isolated from the total scattering by plotting  $I(Q)/T$  vs  $T$ . In Fig. 4 the results are given for Pd-2 at. % Mn and Pd-0.25 at. % Fe. From these figures clear evidence is found for a low-temperature contribution which is not caused by critical scattering originating from thermal fluctuations in the magnetization near the Curie temperature, but which arises as a special property, namely, the presence of clusters in the low-temperature ferromagnetic phase of these dilute alloys. Further evidence for the existence of these clusters comes from the  $Q$  dependence of the small-angle scattering which will be presented in Sec. IIIB.

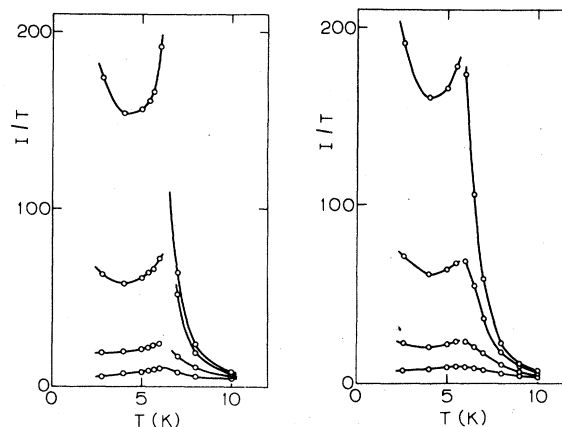


FIG. 4. The scattering intensity divided by temperature ( $I/T$ ) vs temperature for Pd-2 at. % Mn (right) and Pd-0.25 at. % Fe (left). An extra low-temperature contribution is clearly observed. The  $Q$  values are the same as in Figs. 1 and 2, from top to bottom: 0.0246, 0.041, 0.0696, and 0.106  $\text{\AA}^{-1}$ .

In order to investigate the origin of the anomalous low-temperature contribution in the small-angle scattering, measurements have also been carried out with external magnetic fields up to 0.36 T. Since the critical scattering near the ferromagnetic transition originates from large fluctuations in the magnetization which are essentially time dependent, one would expect the critical scattering to be very sensitive to an applied magnetic field, because a magnetic field will diminish the thermally driven fluctuations (reducing the critical scattering) and will favor the spontaneous magnetization which will appear in the magnetic Bragg scattering. In Figs. 5 and 6 typical results are shown of the reduction of the critical scattering upon applying magnetic fields at temperatures in the vicinity of the Curie temperature for Pd-2.1 at. % Mn and Pd-0.5 at. % Fe. These results are in agreement with the above-mentioned qualitative argument for reducing the thermal fluctuations in the magnetization.

The magnetic field dependence of the critical scattering has not received much attention in the literature. A theoretical study within the mean-field approximation for ferromagnetic systems by Villain<sup>16</sup> showed that the scattering intensity in the vicinity of the Curie temperature is a complicated function of the applied magnetic field  $H$ , temperature  $T$ , and the wave vector  $Q$ . Good agreement has been obtained between this calculation and experimental results on the field dependence of the critical scattering in pure iron, illustrating that the inverse critical scattering intensity is proportional to the applied magnetic field ( $I^{-1} \propto H$ ) for small scattering angles. Indeed, a similar behavior is found in the present results on Pd Mn and Pd Fe alloys. A typical example is shown in the

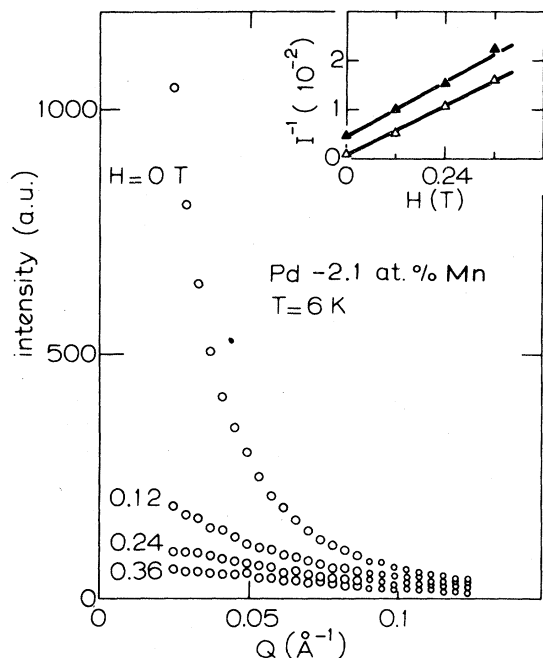


FIG. 5. The critical scattering intensity at  $T=6$  K of Pd-2.1 at.% Mn in various magnetic fields. The reduction is evident from the graph. The insert shows the inverse intensity for  $Q=0.024$  ( $\Delta$ ) and  $0.057$  ( $\blacktriangle$ )  $\text{\AA}^{-1}$  vs magnetic field (Villain relation).

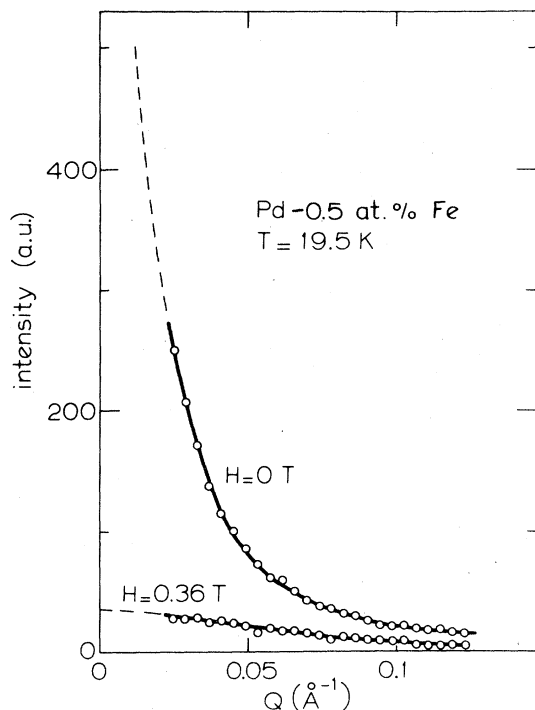


FIG. 6. The critical scattering intensity vs  $Q$  of Pd-0.5 at.% Fe at  $T=19.5$  K in magnetic fields of 0 and 0.36 T. The solid curves represent a fit of the experimental data to a Lorentzian.

insert of Fig. 5 where the inverse intensity of Pd-2.1 at.% Mn for two  $Q$  values is plotted against the applied magnetic field strength, and clearly the data obey the Villain inverse field relation.

The anomalous scattering intensities at low temperatures as a function of the scattering wave vector  $Q$  also show a magnetic field dependence very similar to that of the thermal critical region near  $T_C$ . Typical results for Pd-2 at.% Mn and Pd-0.25 at.% Fe are shown in Figs. 7 and 8 and, once again, a drastic reduction of the scattering intensity is observed. Furthermore, the Villain relation ( $I^{-1} \propto H$ ) is obeyed as shown in the insert of Fig. 8. This result suggests a similar origin of the small-angle scattering in these dilute alloys at the lowest temperatures, as well as in the critical temperature region where the thermal fluctuations cause the large small-angle scattering. Therefore, from the field dependence of the low-temperature small-angle scattering, we propose that static fluctuations in the magnetization (inhomogeneities) due to the random distribution of clusters and/or microdomains cause the enhanced scattering in zero magnetic field. Additional evidence for this point of view comes from the  $Q$  dependence of the scattering.

We can simply describe the field dependence of the intensity in the following way. At low temperatures a random distribution of ferromagnetically correlated regions (clusters or domains) with different orientations gives a strongly  $Q$ -dependent, quasicohherent contribution to the scattering intensity. Upon applying a magnetic field a preferred direction is imposed

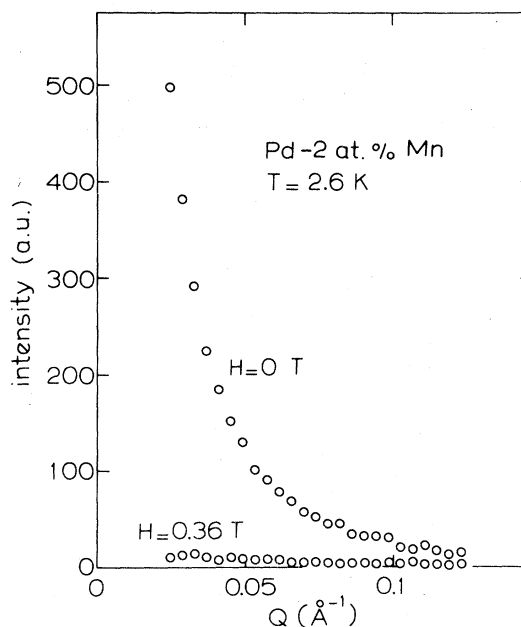


FIG. 7. The scattering intensity at low temperature of Pd-2 at.% Mn vs  $Q$  in magnetic fields of 0 and 0.36 T.

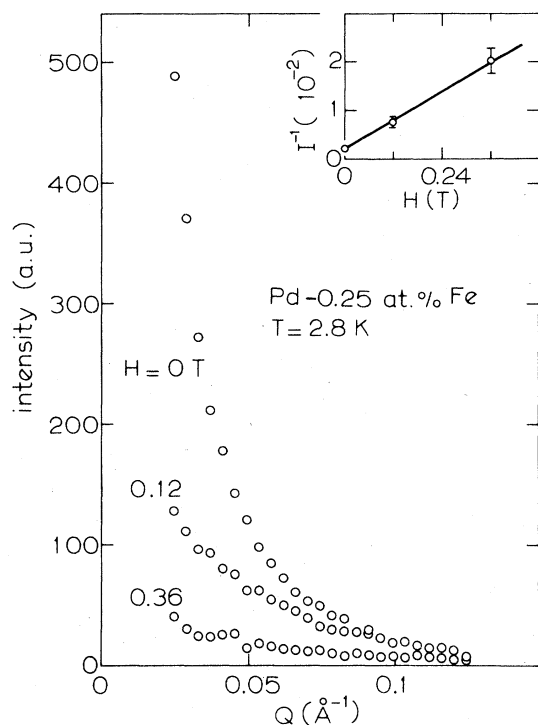


FIG. 8. The scattering at  $T = 2.8$  K of Pd-0.25 at.% Fe vs  $Q$  for various applied magnetic fields. The insert shows the Villain inverse field relation for  $Q = 0.036 \text{ \AA}^{-1}$ .

on the crystal and results in an alignment of the magnetization directions and increases the long-range ferromagnetic order. However, the long-range order contributes to the magnetic Bragg scattering and results in a strong decrease of the quasicohherent scattering.

#### B. $Q$ dependence of the magnetic scattering

Measurements of the  $Q$  dependence of the small-angle neutron scattering intensity lead to information about the spatial correlations between the magnetic moments. A study of the variation of scattering intensity with scattering vector  $Q$ , especially in the vicinity of a magnetic phase transition, is very useful since it gives an insight into the ordering process. The average correlation lengths can be obtained directly from the  $Q$  dependence of the critical scattering intensity determined by the wave-vector-dependent susceptibility  $\chi(Q)$  given by Eqs. (2) and (4).

According to Eq. (2), one obtains a straight line when the reciprocal intensity  $I^{-1}$  is plotted versus  $Q^2$ . From the intercept of  $I^{-1}$  with the vertical axis and the slope of the line the correlation length is readily

calculated. In Figs. 9 and 10 typical scattering data for Pd-2 at.% Mn and Pd-0.25 at.% Fe are presented and, indeed, excellent linear plots are obtained for temperatures above the Curie temperature. The correlation lengths  $\xi = (1/\kappa_1)$  for all alloys for which the temperature dependence has been measured, are calculated from a least-squares fit to the experimental data and are given in Table I. The rapid increase of  $\xi$  as the critical temperature  $T_C$  is approached signals the onset of long-range ferromagnetic order.

However, at temperatures close to and below the Curie temperature deviations from the straight lines are observed. Similar effects have been observed in other random ferromagnetic alloys as for example Co(GaFe) and Co(GaMn),<sup>17</sup> AuFe,<sup>18</sup> CrFe,<sup>19</sup> and PdFeMn.<sup>20</sup> Although no clear explanation exists for this behavior of the small-angle scattering in the low-temperature phase of random ferromagnetic alloys, a number of attempts have been made to attribute this tendency to an additional  $Q^4$  dependence, originating from magnetic assemblies, with a Lorentzian form factor<sup>17</sup> or from ramified clusters within the long-ranged ferromagnetic phase.<sup>19</sup> The  $Q^4$  contribution to the scattering intensity in the vicinity of the transition temperature might be obtained from an expansion to second order in  $J(Q)$ , the Fourier transform of the exchange interaction  $J(R)$ .

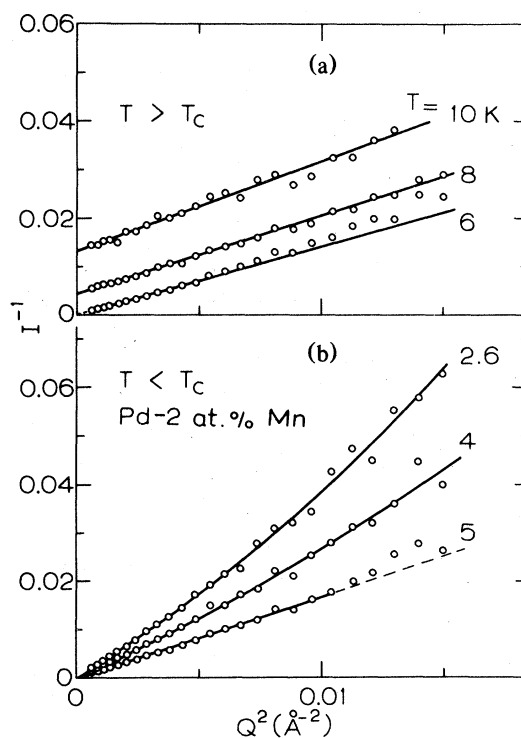


FIG. 9. Reciprocal intensity vs  $Q^2$  Pd-2 at.% Mn for (a)  $T > T_C$  and (b)  $T < T_C$ .

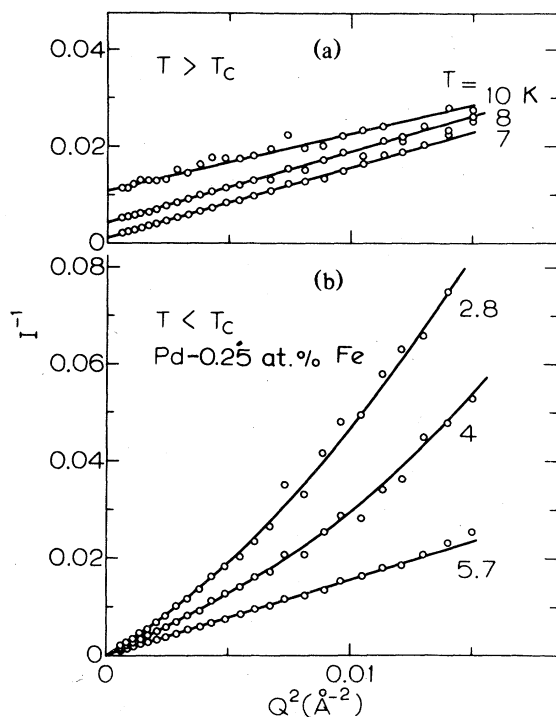


FIG. 10. Reciprocal intensity vs  $Q^2$  for Pd-0.25 at. % Fe for (a)  $T > T_C$  and (b)  $T < T_C$ .

Such an expansion gives

$$J(Q) = J(0) - \frac{1}{6} J^{(2)} Q^2 + \frac{1}{216} J^{(4)} Q^4, \quad (5)$$

where  $J^{(n)} = \sum_{\vec{R}} R^n J(\vec{R})$ . The experimental results for temperatures below the Curie temperature can be well fitted with an extra  $Q^4$  term, however, it is then found that this deviation from the Lorentzian curve increases with decreasing temperature, where one should expect the effect of thermal critical scattering to become unimportant (see, e.g., Sec. III A). Therefore, we believe that this expansion argument is not applicable to the present results and the origin of the observed deviations must lie in the microscopic properties of the ferromagnetic phase of the dilute Pd alloys.

Since the Curie temperatures of the alloys studied are low, it is difficult to separate the thermal critical scattering from any other scattering mechanism present at temperatures  $T \lesssim T_C$ . Nevertheless, we may estimate from Fig. 4 that the thermal critical scattering contribution is very small at the lowest measurement temperature and here the scattering intensity will predominantly be determined by the scattering of static fluctuations in the magnetization due to the random distribution of magnetic giant-moment impurities. Although long-range inhomogeneous ferromagnetic order is established, percolation calculations on lattices show that the infinite

TABLE I. Correlation lengths  $\xi$  obtained from the  $Q$  dependence of the critical scattering for  $T > T_C$ .

<i>PdMn</i> <i>T</i> (K)	0.46 at. % $\xi$ (Å)	<i>PdMn</i> <i>T</i> (K)	2 at. % $\xi$ (Å)
5	$5.8 \pm 0.1$	10	$12.0 \pm 0.2$
2.5	$14 \pm 2$	9	$14.6 \pm 0.2$
	( $T_C = 1.8$ K)	8	$18.9 \pm 0.2$
		7	$35.2 \pm 0.3$
		6.5	$78 \pm 8$
		6	$117 \pm 14$
			( $T_C = 5.7$ K)
<i>PdFe</i> <i>T</i> (K)	0.25 at. % $\xi$ (Å)	<i>PdFe</i> <i>T</i> (K)	0.5 at. % $\xi$ (Å)
10	$10.2 \pm 0.2$	50	$12.3 \pm 0.6$
8	$18.6 \pm 0.2$	35	$15.8 \pm 0.6$
7	$34.5 \pm 0.4$	27.5	$25.5 \pm 0.6$
	( $T_C = 6.5$ K)	25	$33.7 \pm 0.8$
		20	$78 \pm 7$
			( $T_C = 17.5$ K)

cluster(s) can be very ramified<sup>21</sup> and may be broken up in zero magnetic field at the weakest links into smaller randomly orientated ferromagnetic clusters or microdomains due to the shape anisotropy of the clusters. This implies that the small-angle scattering at the lowest temperature is determined by a collection of ferromagnetic microdomains giving rise to a large peak in the forward direction. This explanation is strongly supported by recent neutron scattering experiments on PdFeMn (Ref. 20) where the ferromagnetic coupling has been intentionally weakened by the addition of Mn with its direct antiferromagnetic interaction to the PdFe. For this ternary system a much larger scattering intensity upturn has been observed at the lowest temperatures.

### C. Cluster description

In the following we will employ a model for the small-angle scattering in inhomogeneous ferromagnetic systems based upon the existence of finite ferromagnetic clusters or microdomains with random orientations. This model is analogous to the nuclear small-angle scattering by a large number of arbitrarily shaped particles with random orientations. We will employ a spherical cluster shape as a first approximation since it appears not to be too severe a restriction to the model, and assume an average homogeneous magnetization within the spherical cluster of radius  $R$ . It should be noted that the calculations can be carried out with any shape. The neutron scattering cross section per atom for a collection of ferromagnetic clusters with radius  $R_c$  is then given by

$$\frac{d\sigma}{d\Omega} = \frac{2}{3} \left( \frac{\gamma e^2}{2mc^2} \right)^2 \frac{c'}{n} \mu_{R_c}^2 F_{R_c}^2(\bar{Q}), \quad (6)$$

where  $c'$  is the fraction of magnetic ions in clusters,  $n$  the number of ions in each cluster,  $\mu_{R_c}$  is the total magnetic moment of the cluster, and  $F_{R_c}(\bar{Q})$  the magnetic form factor of the cluster which is given with the above-mentioned assumptions by the Fourier transform of the cluster form function  $f(\bar{r})$ :

$$\begin{aligned} F(\bar{Q}) &= \int_{\text{sphere}} f(\bar{r}) \exp(-i\bar{Q}\cdot\bar{r}) d\bar{r} \\ &= \frac{3}{R_c^3} \int_0^{R_c} dr r^2 \frac{\sin(Qr)}{Qr} \\ &= 3 \frac{\sin(QR_c) - QR_c \cos(QR_c)}{(QR_c)^3}, \end{aligned} \quad (7)$$

where the normalization constant is chosen such that  $F(\bar{0}) = 1$ . In Fig. 11 the form factor  $F(\bar{Q})$  is plotted against the scattering vector  $\bar{Q}$  for various cluster radii. This figure clearly demonstrates that large clusters give narrow peaks, and thus a strongly  $Q$ -

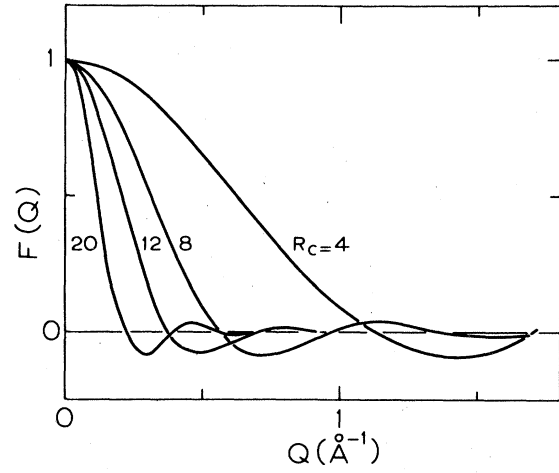


FIG. 11. Form factor of a cluster with various radii  $R_c$  ( $\text{\AA}$ ) vs scattering vector  $\bar{Q}$ .

dependent small-angle scattering. It can further be shown<sup>22,23</sup> that the central region of the peak is related to a geometrical parameter of the scattering object, independent of the shape of the object. The approximated average scattering intensity for small  $Q$  values is given by

$$I(Q) \propto \mu_{R_c}^2 \exp\left(-\frac{1}{3}R^2Q^2\right), \quad (8)$$

where  $R^2$  is the radius of gyration of the scattering object—called the Guinier radius—and for a sphere  $R^2 = \frac{3}{5}R_c^2$ . If the small-angle scattering of the Pd-based alloys at low temperatures is determined by a collection of identical ferromagnetic clusters, then a  $\log I$  vs  $Q^2$  plot would result in a straight line. This, however, is not observed experimentally. Instead, the  $\log I$  vs  $Q^2$  shows a pronounced curvature throughout the  $Q$  region and this deviation must be taken as evidence for a distribution of cluster sizes.<sup>23</sup> Within the Guinier region [Eq. (8)] the scattering intensity is now given by

$$I(Q) \propto \sum_k g_k \mu_k^2 \exp\left(-\frac{1}{3}R_k^2Q^2\right), \quad (9)$$

where  $\mu_k$  is the magnetic moment of a cluster with radius of gyration  $R_k$  and a probability factor  $g_k$ . The scattering intensity is not an exponential curve anymore, but for small  $Q$ ,  $I(Q)$  can be approximated by

$$I(Q) \approx \sum_k g_k \mu_k^2 \left(1 - \frac{1}{3}R_k^2Q^2 + \dots\right), \quad (10)$$

where

$$R_m^2 = \frac{\sum_k g_k \mu_k^2 R_k^2}{\sum_k g_k \mu_k^2} \quad (11)$$

is the weighted average radius of gyration. It must be noted that in calculating this average the largest clusters contribute much more than the smaller ones. Equation (9) can be written in a general normalized form as

$$I(Q) \propto \frac{\sum_k g_k \mu_k^2 F_k^2(Q)}{\sum_k g_k \mu_k^2} \quad (12)$$

In principle the distribution function  $g_k$  can be obtained from a Fourier transform of the experimental intensity curve, providing all clusters have the same composition and a known shape. In practice this procedure rarely works well because of a limited experimental  $Q$  range.<sup>22,24,25</sup> Therefore, we have calculated scattering intensity curves firstly assuming a uniform distribution of cluster radii

$$g(R_k) = \begin{cases} 1 & \text{if } R_k < R_{\max} \\ 0 & \text{if } R_k > R_{\max} \end{cases}, \quad (13)$$

giving a one-parameter fit, and secondly with a Gaussian distribution (a two-parameter fit)

$$g(R_k) \propto \exp\left[-\frac{(R_k - \bar{R}_k)^2}{2(\delta \bar{R}_k)^2}\right], \quad (14)$$

where  $\bar{R}_k$  is the average cluster radius of gyration [note that  $\bar{R}_k$  is different from  $R_m$  given by Eq. (11)] and  $\delta$  the relative width of the distribution.

The results of these calculations are shown in Figs. 12 and 13 for Pd-0.27 at. % Fe and Pd-2.1 at. % Mn at the lowest measurement temperature. A good fit to the experimental data has been obtained via the Gaussian distribution using  $\bar{R}_k = 25 \text{ \AA}$  and  $\delta = 1.2$  for Pd Fe, and  $\bar{R}_k = 20 \text{ \AA}$  and  $\delta = 1.5$  for Pd Mn.

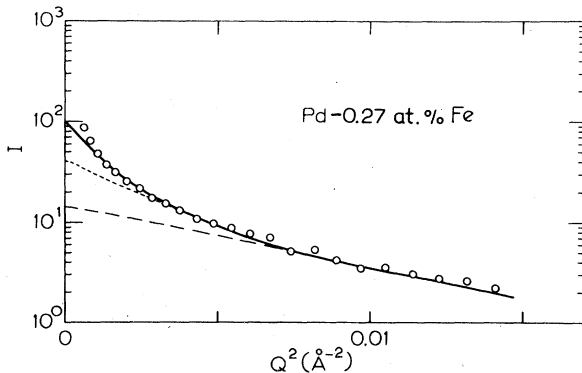


FIG. 12. The scattering intensity  $I$  vs  $Q^2$  of Pd-0.27 at. % Fe at  $T = 2.8 \text{ K}$ . The solid curve is a fit to the data with a Gaussian distribution of radii of gyration ( $\bar{R}_k = 25 \text{ \AA}$  and  $\delta = 1.2$ ). Dotted curve is the fit with the uniform distribution ( $R_{\max} = 50 \text{ \AA}$ ) and the dashed curve is the scattering intensity from a collection of identical clusters with  $R_c = 25 \text{ \AA}$ .

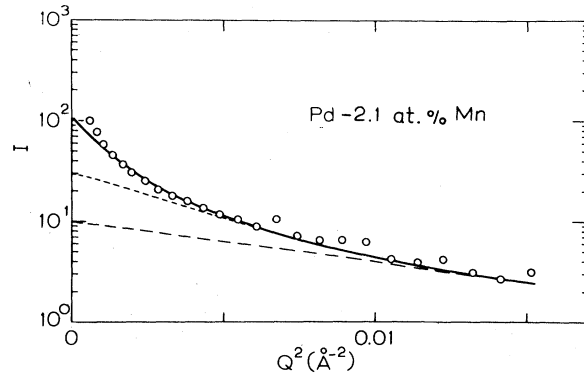


FIG. 13. The scattering intensity  $I$  vs  $Q^2$  of Pd-2.1 at. % Mn at  $T = 2.6 \text{ K}$ . The solid curve is a fit to the data with a Gaussian distribution ( $\bar{R}_k = 20 \text{ \AA}$  and  $\delta = 1.5$ ). The dotted curve is the fit with the uniform distribution ( $R_{\max} = 40 \text{ \AA}$ ) and the dashed curve is the scattering intensity from a collection of identical clusters with  $R_c = 20 \text{ \AA}$ .

The scattering intensity calculated with the uniform cluster radius distribution and an average value  $\bar{R}_k = 25$  and  $20 \text{ \AA}$  is given by the dotted curves in Figs. 12 and 13 and agrees very well with the experiments for  $Q^2 > 0.05 \text{ \AA}^{-2}$ . There are, however, deviations for smaller  $Q$  values because the uniform distribution is apparently inadequate to take into account the presence of (a few) very large clusters. This drawback is overcome by the Gaussian distribution function where the probability of large clusters is given by the tail of the distribution. Clearly such large clusters are present in the alloys since the scattering intensity shows a strong upward curvature at very small  $Q$  values. The scattering intensity cannot be described by a collection of clusters of the same size ( $\delta = 0$ ) as is shown by the dashed curves in Figs. 12 and 13.

In summary, we have found that a distribution of cluster sizes is important to describe the experimental small-angle neutron scattering from inhomogeneous ferromagnetic systems. Nevertheless, the good fits with a Gaussian distribution function do not imply that a Gaussian distribution of spherical clusters is the correct description of the low-temperature phase of the Pd-based alloys. Instead, we feel that similar good results may be obtained from any other distribution function which, in some way, takes into account the large clusters.

#### IV. MAGNETIC DIFFUSE SCATTERING AND MAGNETIZATION

##### A. Anisotropic magnetic scattering

In this section we present the results of the magnetic anisotropic small-angle scattering at low tem-

peratures from ferromagnetic Pd Fe alloys with concentrations of 0.27, 0.48, 0.95, and 2.2 at. % in which high magnetic polarization has been achieved by applying a magnetic field of 0.36 T.

In the preceding sections evidence has been found that the magnetic diffuse scattering in zero magnetic field includes a large contribution from randomly orientated ferromagnetic clusters and domains. Obviously, this "quasicoherent" scattering severely hinders the observation of the diffuse scattering from the giant moments which are associated with the individual impurity moments. However, we also have seen that a magnetic field of 0.36 T was sufficient to annul the small-angle scattering. The field probably aligns the clusters and thereby suppresses the scattering from these static fluctuations in the magnetization, as well as, the thermal critical scattering from dynamic fluctuations.

The ordinary type of diffuse magnetic scattering, which can be compared for  $Q = 0$  with magnetization measurements, can be separated from the total scattering because of its anisotropic character in a magnetic field.

The anisotropic magnetic scattering intensities are very small compared to the total isotropic background scattering and, therefore, these magnetic contributions have been determined in two ways. The intensity of a pure Pd sample of the same size has also been measured and, since the incoherent scattering of Pd is negligible, it is, apart from the attenuation of the beam by absorption, comparable to an empty sample holder measurement. The empty sample holder and the pure Pd background measurements are in general agreement with each other, when the previously quoted value for the absorption cross section in Pd ( $5.2 \pm 0.5$  b at  $\lambda = 1.8 \text{ \AA}$ ) is used. The correctness of this value has been confirmed by independent transmission experiments on the same samples at neutron wavelengths of 2.58 and 4.04  $\text{\AA}$ . The magnetic intensities were obtained by averaging the results of both methods.

The diffuse magnetic cross section for a dilute ferromagnetic alloy one of whose components is non-magnetic is given by<sup>8,14</sup>

$$\frac{d\sigma}{d\Omega} = N \left( \frac{\gamma e^2}{2mc^2} \right)^2 (1 - \cos^2\alpha) T(\vec{Q}) , \quad (15)$$

with

$$T(\vec{Q}) = c(1-c) [F_{\text{imp}}(\vec{Q})\mu_{\text{imp}} + F_{\text{host}}(\vec{Q})H(\vec{Q})]^2 , \quad (16)$$

where  $\alpha$  is the angle between the scattering vector  $\vec{Q}$  and the magnetic-moment direction,  $F_{\text{imp}}(\vec{Q})$  and  $F_{\text{host}}(\vec{Q})$  are the magnetic form factors of the impurity and host magnetization,  $H(\vec{Q})$  represents the induced polarization around the magnetic moment, and

$(\gamma e^2/2mc^2)^2$  has a value of 72.9 mb. The factor  $(1 - \cos^2\alpha)$  enables one to separate the magnetic contribution from the isotropic nuclear and background scattering by applying a magnetic field. Therefore, the geometry of the two-dimensional detector allows a direct measurement of the anisotropic magnetic contribution to the scattering within the detector plane. The magnetic scattering was evaluated from the total scattering intensity by performing a least-squares fit of the observed scattering (after corrections have been made for detector efficiency and the background) to the function

$$I(R_i, \alpha) = A(R_i) + B(R_i) \cos^2\alpha , \quad (17)$$

where  $R_i$  represents the radial distance from the center of the beam to the  $i$ th detector element and  $\alpha$  is the angle between a radial line to that element and the horizontal magnetic field direction. The parameter  $B(R_i)$  is negative and is determined by the magnetic scattering, whereas the isotropic scattering parameter  $A(R_i)$  contains both the nuclear as well as the magnetic scattering. A typical example of the anisotropic scattering intensity is shown in Fig. 14 for Pd-0.48 at. % Fe at  $T = 3.3$  K, and, indeed, the experimental data obey Eq. (17) reasonably well.

The magnetic scattering intensities have been calibrated with the incoherent scattering intensity of a 3-mm-thick vanadium plate. The magnetic moments are then calculated using the ferromagnetic cross sec-

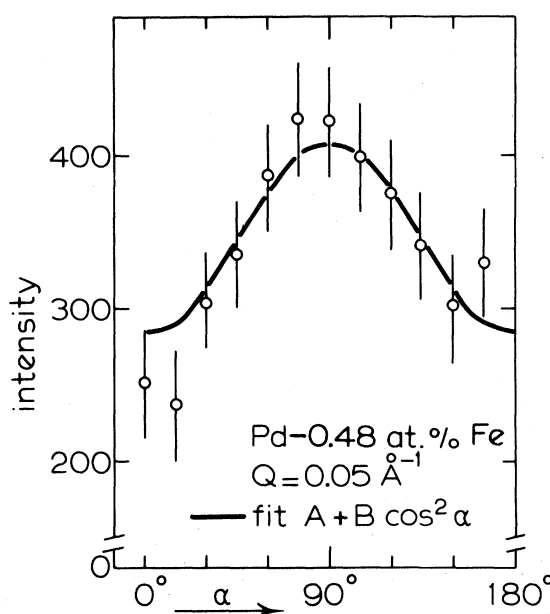


FIG. 14. The total scattering intensity of Pd-0.48 at. % Fe vs the angle  $\alpha$  between the scattering vector  $\vec{Q}$  and applied field direction.

tion, Eq. (15)

$$\frac{d\sigma}{d\Omega} = \left( \frac{\gamma e^2}{2mc^2} \right)^2 [F(\vec{Q})\mu]^2 \quad (18)$$

Since in our  $Q$  range we may set  $F(Q) = 1$  this equation reduces to the simple expression  $d\sigma/d\Omega = 0.0729\mu^2$  (b/sr atom).

In Fig. 15 the magnetization  $M$  as a function of scattering vector expressed in  $\mu_B/\text{atom}$  is shown for all the investigated  $Pd$  Fe alloys. All alloys, except for the lowest concentration, show a rather flat  $Q$  dependence which is characteristic for the  $3d$  form factor of the impurities, but different from the diffuse magnetic scattering results in zero magnetic field obtained by Low and others.<sup>8,9</sup> In view of the preceding section on the zero-field scattering results we must conclude that the analysis of these earlier measurements on  $Pd$  Fe are, in view of their large  $Q$  values and poor  $Q$  resolution, probably hampered by the contribution from clusters and domains in the small-angle region, which *cannot* be only attributed to the giant-moment polarization. On the other hand, the present scattering results do not extrapolate

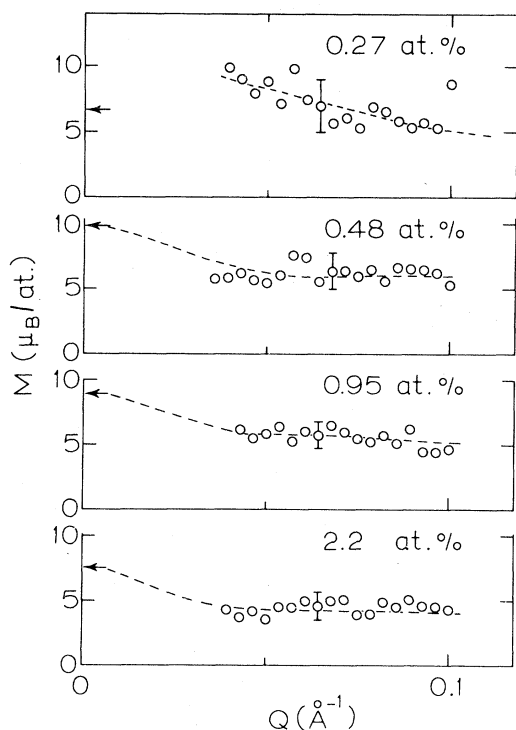


FIG. 15. The  $Q$  dependence of the magnetization obtained from the anisotropic scattering intensities of  $Pd$  Fe alloys. The arrows indicate the value of the magnetization as obtained from macroscopic magnetization measurements at the same temperatures and magnetic fields as used in the neutron experiments.

linearly to the  $Q = 0$  value determined by the magnetization of the alloys, (see next section) indicated by the arrows in Fig. 15. This would suggest a nonuniform spatial distribution of the magnetization per impurity with an average correlation length of order 50 Å.

The  $Pd$ -0.27 at. % Fe alloy shows an enhanced scattering in the forward direction as compared to the magnetization ( $Q = 0$ ) which is similar to the earlier neutron scattering results on  $Pd$  Mn alloys.<sup>10,11</sup> In the present measurements this enhancement is probably related to the incomplete magnetic saturation, and we would suggest that an extra contribution to the scattering results from a few nonaligned clusters. A similar effect was observed much stronger in the  $Pd$  Mn experiment since these latter measurements had essentially been performed in zero magnetic field.

## B. Magnetization measurements

Magnetization measurements have been carried out with a vibrating sample magnetometer (PAR type 155) on small spherical pieces cut from the same samples as used in the neutron scattering experiments. These samples have been measured in magnetic fields up to 1.2 T at the same temperatures at which the neutron experiments were performed. The results for the magnetization are shown in Figs. 16 and 17, where the impurity magnetization is plotted versus magnetic field for all alloys. The magnetization data have been corrected for the  $Pd$ -host magnetization by using the susceptibility value  $\chi_{Pd} = 6.85 \times 10^{-6}$  emu/g. The arrows indicate the

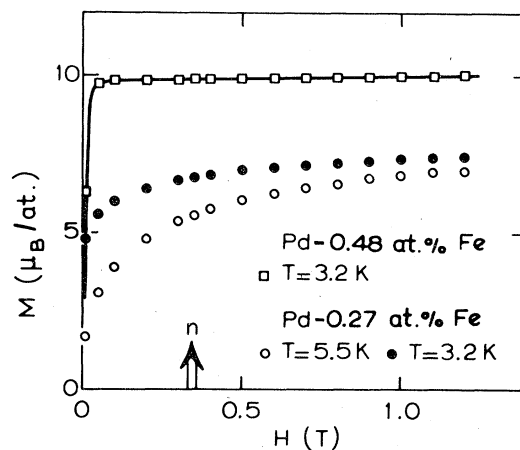


FIG. 16. Impurity magnetization of  $Pd$  Fe 0.27 and 0.48 at. % as function of magnetic field. The arrow indicates the magnetic field for which the neutron measurements have been performed.

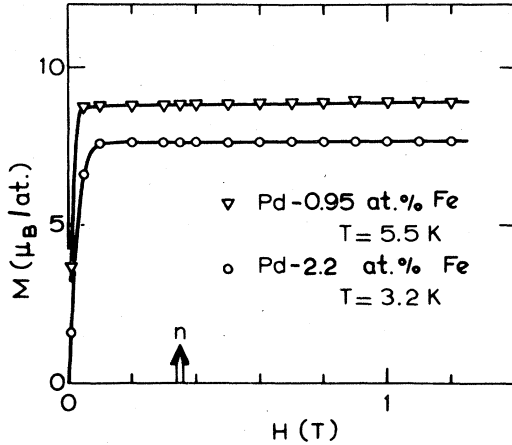


FIG. 17. Impurity magnetization of Pd-Fe 0.95 and 2.2 at. % as function of magnetic field. The arrow indicates the magnetic field used in the neutron experiments.

magnetic field value of the neutron experiments. Again, in the magnetization, a marked difference in the magnetic behavior is observed between the Pd-0.27 at. % Fe and the more concentrated alloys. The latter alloys show a normal ferromagnetic behavior and already saturate in rather small fields. The Pd-0.27 at. % Fe alloy shows a rather peculiar magnetization, no well-defined knee is observed and saturation is not achieved in fields up to 1.2 T. Such magnetization behavior is very similar to magnetization results on dilute Pd-Co alloys,<sup>3</sup> and this has been ascribed to the large width of the ferromagnetic transition. Such an interpretation agrees with the present neutron results in that magnetic clusters are expected to grow in a wide temperature range due to the random distribution of impurities in the host. The same concentration dependent magnetic behavior in Pd-Fe alloys with concentrations below 0.3 at. % Fe has also been observed by other magnetization measurements.<sup>26</sup> Furthermore, the nuclear-spin-lattice relaxation rates in Pd-Fe alloys<sup>27</sup> show a strong decrease for concentrations  $c < 0.5$  at. % for which no proper explanation could be given.

We therefore feel that a systematic, magnetic, and lattice-structure study of Pd-Fe alloys with concentration up to 0.5 at. % is necessary to understand the peculiar magnetism of these low-concentration alloys. The structural properties may be of importance since the lattice expands unusually with increasing amount of Fe and has a maximum for  $c \approx 0.3$  at. %.<sup>28</sup>

#### V. FERROMAGNETIC ORDERING IN DILUTE ALLOYS AND PERCOLATION

The existence of giant moments in Pd alloys is one of the conditions for ferromagnetic ordering in alloys

with concentrations much less than a critical concentration for direct interactions between the magnetic impurities. Obviously, the conduction or band electrons provide the coupling between the giant moments as well as being polarized into the giant moments. A simple description of the static properties of giant moments in Pd can be obtained within the linear-response approximation by assuming that the bare magnetic moment polarizes the surrounding electrons of Pd, and that the polarization, as a function of distance, is determined by the generalized magnetic susceptibility of the Pd host.

If the host were a normal metal in which the conduction electrons could be treated as free electrons, this susceptibility  $\chi(r)$  would be determined by the RKKY (Ruderman-Kittel-Kasuya-Yosida) interaction which is oscillatory and of infinite range, if mean-free-path effects are neglected. Here, no significant net polarization would be present, because the spatial integral of  $\chi(r)$  approximates zero. However, if the Coulomb interaction between the band electrons (i.e., the intra-atomic exchange interaction) is important as in the case of Pd, it will enhance the spin susceptibility of the electron gas leading to the exchange enhanced susceptibility given according to the random-phase approximation<sup>29</sup> as

$$\chi(q) = \chi_{\text{RKKY}}(q) / [1 - \bar{I}\chi_{\text{RKKY}}(q)] \quad (19)$$

where  $\chi_{\text{RKKY}}(q)$  is the Fourier transform of the RKKY interaction function and  $\bar{I}$  is a measure for the strength of the Coulomb intra-atomic interaction. Since  $\chi_{\text{RKKY}}(q)$  is a monotonically decreasing function with increasing  $q$ ,  $\chi_{\text{RKKY}}(q)$  is more enhanced at low values of  $q$  than at higher  $q$  values. This selective enhancement at low  $q$  increases the range of interactions and causes an extra net polarization in the host metal which creates the giant moment. An important result is that the first node in  $\chi(r)$  obtained from Eq. (19) appears at a much larger distance than in the pure RKKY case. This means that in alloys for which the average distance between the impurities is smaller than the first node distance, the interactions are now predominantly positive, leading to a ferromagnetic type of ordering. Only at large mean distances (i.e., very low concentrations) can the oscillatory character of the interaction produce a spin-glass phase.<sup>30,31</sup>

The general concept of percolation has widely been applied to the problem of dilute ferromagnetic systems in which direct interactions between the magnetic ions determine the magnetic behavior.<sup>32,33</sup> The percolation limit,  $c_p$ , in a dilute ferromagnetic system is the lower bound to the concentration of spins required for a cluster of infinite size, i.e., the occurrence of a ferromagnetic phase transition. In addition to the infinite cluster(s) a large number of finite clusters coexist for concentrations just above  $c_p$ . If the interactions between the spins are short ranged

(e.g., only a first-nearest-neighbor distance) the percolation limit strongly depends upon the lattice structure. But for longer-ranged interactions the detailed lattice structure becomes less important. The critical concentration  $c_p$  then depends mainly on the coordination number  $z$ , which is defined as the number of bonds to each lattice site. An asymptotic approximation of the critical concentration for large coordination number  $z$  in three-dimensional lattices is  $c_p \approx 2.7/z$ .<sup>34</sup>

In the spin-glass problem the concept of percolation has been introduced by Smith<sup>4,5</sup> in order to give a qualitative description of the magnetic clustering and the zero-field susceptibility behavior. Since the RKKY interaction and its exchange enhanced form are long ranged and decay approximately as  $1/r^3$ , magnetic ordering can now be obtained for any concentration by sufficiently lowering the temperature. A magnetic cluster is defined as a group of spins each of which is coupled to at least one other member of the group by an exchange bond stronger than the thermal energy. This definition does not necessarily mean that the spins in the cluster are all ferromagnetically coupled, but a spin in a cluster is aligned according to the internal field produced by its neighboring spins. In addition to the strongly coupled spins there are two types of "loose" spins. The first are those spins which are rather isolated in the lattice due to the random distribution of impurities, and have only a weak interaction with other spins. The second type are loose spins embedded in the cluster, but which due to a cancellation of the interactions from various neighboring spins experience a small or zero internal field.

A bond length  $R_b$  of a spin can be defined such that the interaction energy  $J_{\text{RKKY}}(R_b)$  is of the same order of magnitude as the thermal energy  $k_B T$ . Hence, the bond length  $R_b$  is strongly temperature dependent and the clusters will grow with decreasing temperature. The coordination number of a spin in a cluster is for large  $R_b$  given by

$$z = 4\pi R_b^3 / 3\nu_0 \quad (20)$$

where  $\nu_0$  is the atomic volume. Using the asymptotic relation  $c_p \approx 2.7/z$ , the percolation concentration is related to the bond length  $R_b$  by

$$c_p \approx 0.64\nu_0/R_b^3 \quad (21)$$

With this relation it is easy to see why order in dilute alloys is obtained at very low concentrations in Pd alloys. Because the bond lengths  $R_b$  are enlarged due to the exchange enhanced susceptibility of the Pd host,  $c_p$  is small. Recently, a critical concentration has been obtained for the onset of ferromagnetism in Pd Fe alloys by analyzing the available experimental data within a framework based upon the Landau theory of phase transitions.<sup>35</sup> A critical concentration

$c_p = 0.0012$  was obtained, and this corresponds, via Eq. (21), to an average bond length of about 20 Å which is consistent with the average distance between the Fe impurities for this concentration  $\approx 17$  Å.

The properties of dilute alloys with concentrations just above the percolation concentration are thus determined by the infinite cluster and the many finite clusters. The onset of long-range order is established by the infinite cluster in which the fluctuations lead to *thermal critical behavior* and are observed at fixed concentration by varying the temperature. On the other hand, the finite clusters determine the static inhomogeneity of the alloy, and as a function of concentration lead to *geometrical* (or static) *critical behavior* which can also be studied<sup>36,37</sup> in alloys below  $c_p$ .

The ferromagnetic ordering process in dilute Pd based alloys can be described in terms of bond lengths in a way very similar to the freezing process of the spin-glasses.<sup>1,4</sup> This is visualized schematically in Fig. 18. Here a Pd-1 at. % Fe alloy in a two-dimensional lattice is computer simulated. The impurities are randomly distributed in the lattice and periodic-boundary conditions have been applied. The magnitude of the interaction bonds is related to the induced magnetic polarization as given in Fig. 19. The contours of equal magnetization (or bond lengths) in Fig. 18 create a strongly inhomogeneous distribution of magnetization in the lattice. From this figure the ferromagnetic ordering in the alloy can be followed as function of temperature. At high temperatures the exchange interaction is insufficient to

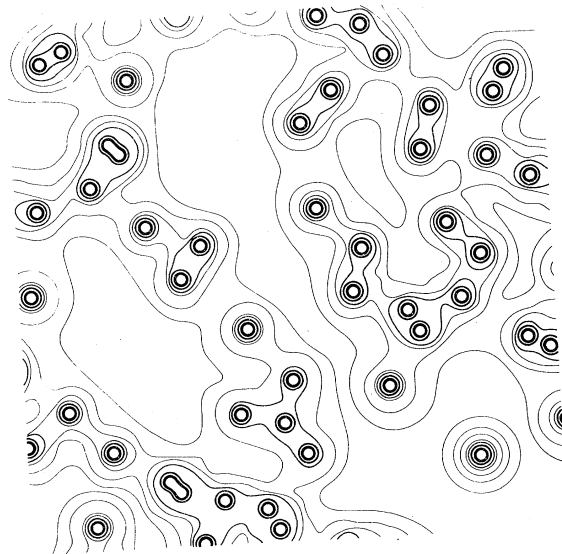


FIG. 18. A computer simulation of the distribution of Fe impurities in a two-dimensional Pd-1 at. % Fe alloy in which contours of equal induced magnetization are shown.

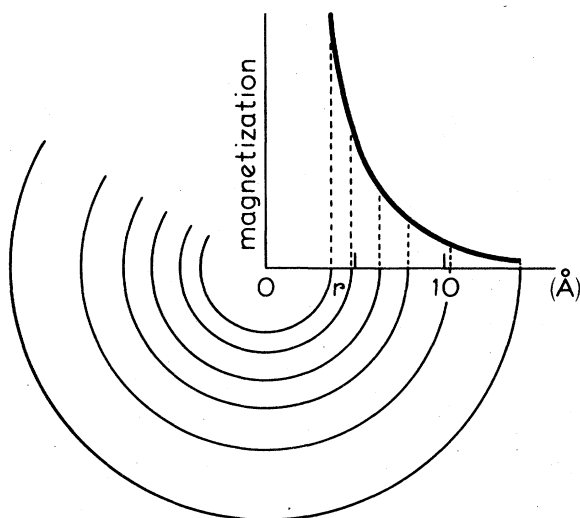


FIG. 19. Contours of equal magnetization in the Pd host around an impurity atom placed in the origin.

overcome the thermal energy  $k_B T$  and the system is in the paramagnetic phase. At lower temperatures, but still above the Curie temperature  $T_C$ , those impurities with exchange interactions larger than the thermal energy will be coupled and form dynamic ferromagnetic clusters. As  $T$  approaches  $T_C$  the ferromagnetic clusters grow because of the increase of the bond length  $R_b$ , and at  $T_C$  the first infinite cluster is formed. However, in contrast to an infinite cluster with short-range interactions, now the magnetization within the infinite cluster is not completely homogeneous, but is made up from large, static agglomerates of clusters. Furthermore, the infinite cluster is composed of a so-called "backbone" and a large number of "tag ends" which behave rather like the additionally present, finite clusters because they feel the exchange field only at one external end. These "tag ends" provide the shape anisotropy by which the magnetization of the clusters or microdomains have different orientations as observed in the present neutron results. For  $T < T_C$  the infinite cluster grows at the expense of the finite clusters, and at  $T = 0$  an inhomogeneous ferromagnetically ordered state appears.

## VI. CONCLUSIONS

Small-angle neutron scattering has been employed to study the magnetic behavior in dilute Pd-based alloys. The measurements showed two distinct scattering contributions as a function of temperature. First, critical scattering has clearly been observed near the

Curie temperature and the intensities could be analyzed for  $T > T_C$  with the usual Ornstein-Zernike formalism. Secondly, for temperatures below  $T_C$ , deviations from the Ornstein-Zernike behavior indicated an extra quasicohherent scattering associated with the inhomogeneous character of the ferromagnetic phase. Both scattering contributions are very sensitive to an applied magnetic field. This effect has been explained by a reduction of the fluctuations in the magnetization for  $T \approx T_C$ , and by an alignment of the ferromagnetic clusters or microdomains for  $T \ll T_C$ . By taking into account this behavior of the diffuse scattering in a magnetic field, one can explain the anomalous small-angle scattering in the earlier studies on Pd Mn as being due to critical scattering. The field-difference counting technique employed in these measurements and previously used by Low *et al.* is, therefore, not suitable for inhomogeneous ferromagnetic systems near or below the transition temperature.

The anisotropy of the magnetic diffuse scattering in a magnetic field has been exploited to determine the magnetic scattering associated with the giant moments of some Pd Fe alloys. The average spatial extent of the induced polarization has been estimated to be about 50 Å. Also the induced polarization per impurity atom decreased with increasing concentration in agreement with macroscopic magnetization measurements. However, a different behavior in both magnetization and magnetic scattering has been found for Pd-0.27 at. % Fe which is still unresolved. In view of these systematic deviations, we suggest further magnetic and lattice-structure studies of Pd Fe alloys for  $c \leq 0.3$  at. %.

The  $Q$  dependence of the small-angle scattering for  $T \ll T_C$  of Pd Fe and Pd Mn alloys could be satisfactorily described by a model which includes a distribution of ferromagnetic clusters with different sizes. The presence of such clusters is a basic property of random alloys. This result has been used to emphasize the similarity between the ferromagnetic ordering in Pd based alloys and the more general spin-glass ordering in which the concept of percolation provides a useful description.

## ACKNOWLEDGMENTS

The authors gratefully acknowledge Dr. A. P. Murani for his interest and cooperation in this work, and the staff of the Institute Laue-Langevin, Grenoble where most of the experiments were performed. We wish to thank Dr. H. van Kempen and Mr. C. Beers of the Katholieke Universiteit Nijmegen for their assistance with the magnetization measurements. The present work is part of the research program of the Nederlandse Stichting voor Fundamenteel Onderzoek der Materie (FOM).

- \*Present address: Philips Research Laboratories, Eindhoven, The Netherlands.
- <sup>1</sup>For a review of the experimental properties of dilute alloys see J. A. Mydosh and G. J. Nieuwenhuys, in *Handbook of Ferromagnetic Materials*, edited by E. P. Wohlfarth (North-Holland, Amsterdam, 1980), Vol. 1, Chap. 2.
- <sup>2</sup>K. H. Fisher, *Phys. Rep.* **47**, 225 (1978).
- <sup>3</sup>G. J. Nieuwenhuys, *Adv. Phys.* **24**, 515 (1975).
- <sup>4</sup>D. A. Smith, *J. Phys. F* **4**, L266 (1974).
- <sup>5</sup>D. A. Smith, *J. Phys. F* **5**, 2148 (1975).
- <sup>6</sup>M. F. Collins and G. G. Low, *Proc. Phys. Soc. London* **86**, 535 (1965).
- <sup>7</sup>R. A. Medina and J. W. Cable, *Phys. Rev. B* **15**, 1539 (1977).
- <sup>8</sup>G. G. Low and T. M. Holden, *Proc. Phys. Soc. London* **89**, 119 (1966).
- <sup>9</sup>T. J. Hicks, T. M. Holden, and G. G. Low, *J. Phys. C* **1**, 528 (1968).
- <sup>10</sup>C. J. de Pater, C. van Dijk, and G. J. Nieuwenhuys, *J. Phys. F* **5**, L58 (1975).
- <sup>11</sup>B. H. Verbeek, T. Amundsen, and C. van Dijk, *Physica (Utrecht)* **86-88B**, 482 (1977).
- <sup>12</sup>B. H. Verbeek, C. van Dijk, B. D. Rainford, and A. P. Murani, *J. Appl. Crystallogr.* **11**, 637 (1978).
- <sup>13</sup>G. E. Bacon, *Neutron Scattering* (Butterworths, London, 1977).
- <sup>14</sup>W. Marshall and S. W. Lovesey, *Theory of Thermal Neutron Scattering* (Clarendon, Oxford, 1971).
- <sup>15</sup>J. Kopp, *J. Phys. F* **3**, 1994 (1973).
- <sup>16</sup>J. Villain, *J. Phys. (Paris)* **24**, 622 (1963).
- <sup>17</sup>R. Cywinski, J. G. Booth, and B. D. Rainford, *J. Appl. Crystallogr.* **11**, 641 (1978).
- <sup>18</sup>A. P. Murani, S. Roth, P. Radhakrishna, B. D. Rainford, B. R. Coles, K. Ibel, G. Schoeltz, and F. Mezei, *J. Phys. F* **6**, 425 (1976).
- <sup>19</sup>S. K. Burke, R. Cywinski, and B. D. Rainford, *J. Appl. Crystallogr.* **11**, 644 (1978).
- <sup>20</sup>S. M. Shapiro, G. Shirane, B. H. Verbeek, G. J. Nieuwenhuys, and J. A. Mydosh, *Solid State Commun.* (in press).
- <sup>21</sup>H. E. Stanley, R. J. Birgeneau, P. J. Reynolds, and J. F. Nicoll, *J. Phys. C* **9**, L553 (1976).
- <sup>22</sup>A. Guinier and G. Fournet, *Small-angle Scattering of X-rays* (Wiley, New York, 1955).
- <sup>23</sup>A. Guinier, *X-Ray Diffraction* (Freeman, San Francisco, 1963).
- <sup>24</sup>J. Schelten and R. W. Hendricks, *J. Appl. Crystallogr.* **11**, 297 (1978).
- <sup>25</sup>I. S. Fedorova and P. W. Schmidt, *J. Appl. Crystallogr.* **11**, 405 (1978).
- <sup>26</sup>Note the different saturation magnetization in: J. Crangle and W. R. Scott, *J. Appl. Phys.* **36**, 921 (1965), G. Chouteau and R. Tournier, *J. Phys. (Paris)* **32**, C1-1002 (1971); A. J. Manuel and M. McDougald, *J. Phys. C* **3**, 147 (1970).
- <sup>27</sup>M. Sablik, S. Skalski, and J. I. Budnick, *Phys. Rev. B* **8**, 2222 (1973).
- <sup>28</sup>G. Biehl and B. Flanagan, *Solid State Commun.* **28**, 751 (1978).
- <sup>29</sup>C. Kittel, in *Solid State Physics*, edited by F. Seitz, D. Turnbull, and H. Ehrenreich (Academic, New York, 1968), Vol. 22, p. 1.
- <sup>30</sup>G. Chouteau and R. Tournier, *J. Phys. (Paris)* **32**, C1-1002 (1971).
- <sup>31</sup>K. Nagamine, N. Nishida, S. Nagamiya, O. Hashimoto, and T. Yamazaki, *Phys. Rev. Lett.* **38**, 99 (1977).
- <sup>32</sup>J. W. Essam, in *Phase Transitions and Critical Phenomena*, edited by C. Domb and M. S. Green (Academic, New York, 1972), Vol. 2, p. 197.
- <sup>33</sup>V. K. S. Shante and S. Kirkpatrick, *Adv. Phys.* **20**, 325 (1971).
- <sup>34</sup>C. Domb and N. W. Dalton, *Proc. Phys. Soc. London* **89**, 856 (1966).
- <sup>35</sup>J. C. Ododo, *Solid State Commun.* **25**, 25 (1978).
- <sup>36</sup>J. C. Ododo and B. D. Rainford, *J. Phys. C* **11**, 533 (1978).
- <sup>37</sup>R. J. Birgeneau, R. A. Cowley, and G. Shirane, *J. Appl. Phys.* **50**, 1788 (1979).